Computers and Concrete, *Vol. 20, No. 2 (2017) 205-214*
DOI: https://doi.org/10.12989/cac.2017.20.2.205

The research on static and dynamic mechanical properties of concrete under the environment of sulfate ion and chlorine ion

Liangxue Nie[*1], Jinyu Xu[1,2a] and Erlei Bai[1b]

[1]*Department of Airfield and Building Engineering, Air Force Engineering University, Xi'an 710038, China*
[2]*College of Mechanics and Civil Architecture, Northwest Polytechnic University, Xi'an 710072, China*

(Received April 19, 2015, Revised April 14, 2017, Accepted April 16, 2017)

Abstract. The Hydraulically driven test system and Φ 100 mm split Hopkinson pressure bar(SHPB) test device were employed to research the quasi-static and dynamic mechanical properties of concrete specimens which has been immersed for 60 days in sodium sulfate (group S1) and sodium chloride (group S2) solution, the evolution of their mass during corrosive period was explored at the same time, and the mechanism of performances lost was analyzed from the microscopic level by using scanning electron microscope. Results of the experimental indicated that: their law of mass both presents the trend of continuous rising during corrosive period, and it increases rapidly on the early days, the mass growth of group S1 and group S2 in first 7 days are 76.78% and 82.82% of their total increment respectively; during the corrosive period, the quasi-static compressive strength of specimens in two groups are significantly decreased, both of which present the trend of increase first and then decrease, the maximum growth rate of group S1 and group S2 are 7.52% and 12.71% respectively, but they are only 76.23% and 82.84% of specimens which under normal environment (group N) on day 60; after immersed for 60 days, there were different decrease to dynamic compressive strength and specific energy absorption, and so as their strain rate sensitivities. So the high salinity environment has a significant effect of weaken the quasi-static and dynamic mechanical performance of concrete.

Keywords: sulfate ion; chlorine ion; mass; strain rate; compressive strength; specific energy absorption

1. Introduction

Concrete has been widely used in the field of architectural structure and its durability is an attractive concept for a long time in that it affects the service life and safety of structures. As we all know, concrete has excellent durability in general, but for the concrete that under the extreme environment, because of the influence of physical, chemical, etc., its durability faces daunting challenges. Among the factors that influence the durability of concrete structures, salt corrosion which occurs frequently in coastal area and saline soil region is particularly prominent. For the buildings such as houses, seaports, large sea bridges and offshore platform facilities, etc., which are located in coastal area, or directly built on sea surface, their main structures have been immersed in seawater, scoured throughout the year, and corroded by Cl^{-1} and SO_4^{2-} in seawater; Concrete structures located in saline soil region, especially the underground structures, are eroded seriously by salt ions. Cl^{-1} can lead to the earlier and more aggravate corrosion of rebar, so is the drop of concrete cover, which results in the initiation of longitudinal cracks; The sulfate penetration brings gypsum corrosion and ettringite corrosion inside the concrete, which results in the expanded destruction of the internal structure of concrete, thus causing a significant weakening of static and dynamic properties.

So far, many scholars have carried out fruitful researches on the impacts of chlorine and sulfate salt on concrete, but it is not difficult to find that the researches in this field mainly focus on the transmission laws of chloride and sulfate ions which inside the concrete (Deby *et al*. 2009, Song and Chen 2011, Ye *et al*. 2017, Yang *et al*. 2017), the transmission models of ions and damage models of concrete (Cho *et al*. 2015, Zuo *et al*. 2017, Tanyildizi 2017, Yin *et al*. 2017, Song *et al*. 2017, Yoon and Nam 2017), the study on static mechanical performance of concrete that after corroded (Cohen and Mather 1991, Türkmen *et al*. 2003, Hossain and Lachemi 2006, Assaad *et al*. 2008, Uysal *et al*. 2012, Chindaprasirt and Chalee 2014, Sharmila and Dhinakaran 2015), the microexamination (Gao *et al*. 2013, Roventi *et al*. 2014, Fei *et al*. 2014) and corrosion mechanism of chloride and sulfate ions on concrete (Dallaire *et al*. 1997, Clifton and Ponnersheim 1994, Crammond 2003, Steinberg 2009, Chindaprasirt and Chalee 2014). But in reality, the service environment of concrete structures is becoming more and more complex. They are subject to dynamic loads during their service period, such as wind load action, earthquake action, impact action and explosion action, etc., thus higher requirements are put forward for the concrete structure under dynamic load. Therefore, it is necessary to study the performance of concrete in saline environment under high strain rates.

∗Corresponding author, Ph.D. Student
E-mail: nieliangxue_kgd@126.com
[a]Professor
[b]Associate Professor

ISSN: 1598-8198 (Print), 1598-818X (Online)

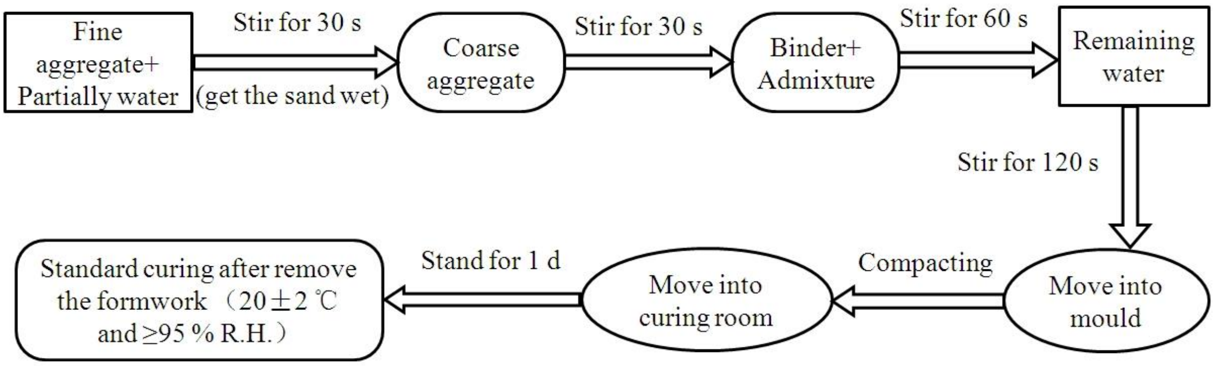

Fig. 1 The casting mechanism of concrete specimens

So based on this phenomenon, the short-term corrosion test was carried out in this paper, the corrosion solutions are $NaCl$ and Na_2SO_4 solutions, both of which are with the mass fraction of 15%, and ensure that the mass fraction of solutions is kept constant during the corrosive period, this experiment adopts immersion corrosion test method for a period of 60 days which is counting from the end of 28-days standard curing. Based on the quasi-static mechanical performance of concrete that after corroded, the quasi-static and dynamic mechanical properties were explored, the evolution of mass during corrosive period were also be studied at the same time, and combined with scanning electron microscope (SEM), the damage mechanism of concrete was analyzed at the micro level. Meanwhile, a control group that doesn't immersed in any solutions, but the external environment were exactly the same, has been set. For the purposes of easy to distinguish, the specimens immersed in the $NaCl$ solution was named as group S1, the specimens immersed in the Na_2SO_4 solution was named as group S2, the control group was named as group N.

2. Experiment

2.1 Materials and specimens

The materials used in the production of concrete specimens are as follows:

Ordinary Portland cement with the strength grade of 42.5R, crushed limestone with unit weight of 2700 kg/m^3 and particle size range of 5-20mm, river sand with unit weight of 2630 kg/m^3 and a fineness modulus of 2.8, tap water, fly ash. The *w/c* of concrete design as 0.54, the mix proportion of concrete is shown in Table 1.

The casting mechanism of concrete specimens can be seen as Fig. 1.

As shown in Fig. 2, there are two kinds of size of concrete specimens were casted in the experiment. The cube specimens with the side length of 100 mm were used for quasi-static test and the evolution of mass during corrosive period, the size depends on Standard for test method of mechanical properties on ordinary concrete (GB/T 50081-2002) (In Chinese). While the cylindrical concrete with the size of 98 mm diameter ×50 mm height

(a) Cube specimen

(b) Cylindrical specimens before polish

(c) Cylindrical specimens after polish

Fig. 2 Concrete specimens

was used for dynamic test, its size depends on the testdevice of Φ 100 mm split Hopkinson pressure bar (SHPB). After 28 days curing, the cylindrical specimens should be polished to ensure that the non-parallelism of specimens is less than 0.02 mm. In addition, their diameter should remain in the scope of 100±1 mm and the thickness should be 50±1 mm.

2.2 Experimental equipment

2.2.1 Quasi-static test

The quasi-static test was based on Standard for test method of mechanical properties on ordinary concrete (GB/T 50081-2002). The device used for quasi-static test is hydraulically driven test system, as shown in Fig. 3(a). This system is mainly composed of hydraulic testing machine, hydraulic source, data acquisition recorder and the computer, and 2000 kN is its maximum load. The compressive strength of concrete is the primary data in the quasi-static test, which was used to explore the capacity of concrete under quasi-static load after attacked.

(a) Hydraulically driven test system

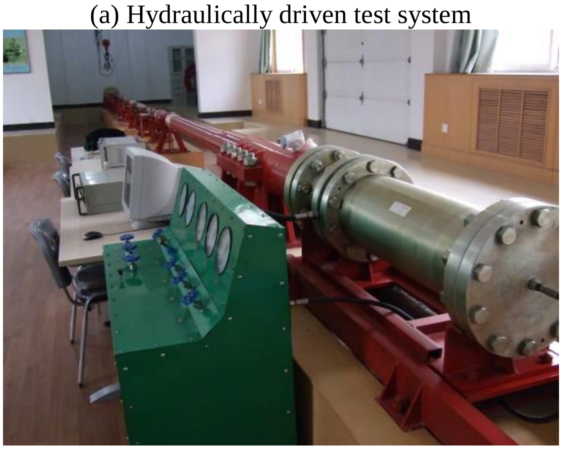

(b) SHPB test device

Fig. 3 Experimental equipment

Table 1 Mix proportions of concrete (kg/m^3)

Cement	Water	River sand	Crushed limestone	Fly ash
338	215	643	1144	60

It is well know that test date of mechanical behavior of concrete shows great discreteness, and with reference to the *Standard*, more than 3 specimens will be tested in each group, and their average is took as the final result. The bottom and top surfaces of hydraulic testing machine and all the surfaces of cube specimen will be cleaned before test, after specimen placed at the center of the bottom surface of hydraulic testing machine, then the quasi-static load applied.

2.2.2 Dynamic test

The split Hopkinson pressure bar (SHPB) device was used in dynamic test, as shown in Fig. 3(b). The SHPB device was composed of main testing equipment, energy systems and date measurement systems. This test device is a very effective equipment to conduct dynamic test, it has a large range of testing strain rate, which makes it possible to study the response of concrete under different levels of dynamic load.

According to the test technique and theory of SHPB (Gama 2014), this dynamic test is based on two assumptions: ① Plane assumption, that is when the stress wave propagating in metal bars, the lateral sections of bars always remain in flat state; ② Stress-homogeneous assumption, that is the stress wave propagates for two round-trip inside the specimen, the stress is equal everywhere inside the specimen. If the interface between metal bar and specimen can't reach the complete consistent state, the stress inside the specimen can't reach the state that completely uniform, thus the experiment can't reach the constant strain rate (Ravichandran and Subhash 1994). If the specimens destroyed under the state of non-constant strain rate, the measured dynamic mechanical properties are not accurate enough. Therefore, the technique of reshape incident waveforms (Frew *et al*. 2002, Lu *et al*. 2002, Li and Xu 2009) has been proposed successively. In this paper, five kinds of pulse shapers, made of H62 brass, with the thickness of 1 mm and the diameter of 20, 22, 25, 27, 30 mm, were used to reshape the waveforms. The experiment has proved that, the waveforms that have been reshaped can meet the requirement of test well, and can ensure the stress inside the specimens reaches the state that completely uniform by eliminate the dispersion effect that result from the spread of rectangular wave in traditional SHPB test.

The dynamic test of concrete also shows great discreteness, so in this test, multiple specimens (at least 3) will be tested at each strain rate. The two surfaces of cylinder specimen, and the surfaces of incident bar and transmission bar, will be cleaned before test, and for the purpose of eliminate the frictional effect cause by the interface of metal bar and specimen, the mixture of graphite and lubricant will be paint on the surface of specimen and bars, after pulse shaper pasted on the center of the other surface of incident bar, then the dynamic load applied.

3. Experimental results and analysis

3.1 Mass changes

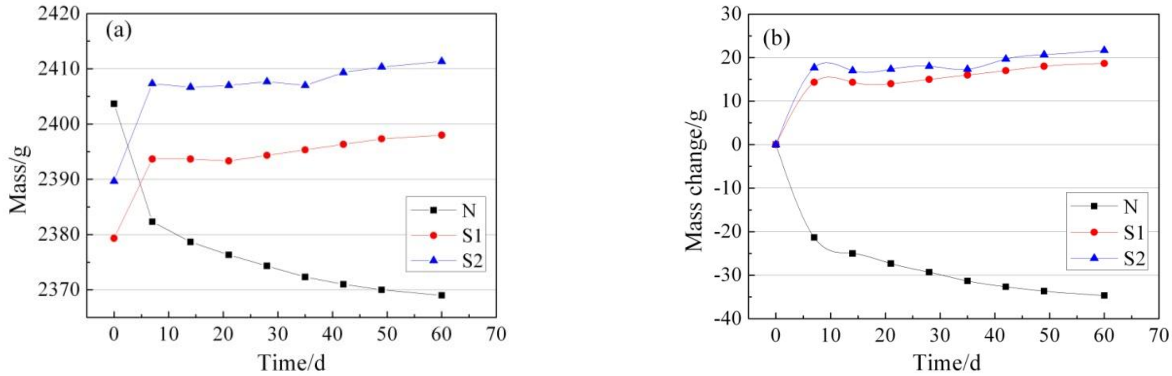

(a) Mass (b) Mass change

Fig. 4 The evolution of mass

Table 2 The mass of concrete during corrosive period (g)

Corrosion time	0 d	7 d	14 d	21 d	28 d	35 d	42d	49d	60 d
N	2403.67	2382.33	2378.67	2376.33	2374.33	2372.33	2371	2370	2369
S1	2379.33	2393.67	2393.67	2393.33	2394.33	2395.33	2396.33	2397.33	2398
S2	2389.67	2407.33	2406.67	2407	2407.67	2407	2409.33	2410.33	2411.33

When the concrete specimens immersed in solutions, the significantly mass change of specimens were result from the influence of two aspects: attacked by salt ions and constantly absorbing water. Although the mass change cannot reflect the corrosion progress of concrete specimens during corrosive period accurately, it is a comprehensive reflection of concrete that after corroded in the macroscopic view.

The mass of cube specimens were weighed every week, and there were several specimens weighed in every group, their average was taken as the final results which shown in Table 2, and its varying tendency with the time was draw which can be seen in Fig. 4. As seen in Table 2 and Fig. 4, with the increase of corrosion time, the mass of specimens in group N decreases gradually, it declines rapidly in the early stage and relatively slow in the late stage, the total loss is 1.44%, and the loss in first 7 days is 61.48 % of the total loss. Distinctive from the specimens in group N, the mass of specimens in group S1 and group S2 increase gradually with the increase of time, and the total increments are 0.79% and 0.91% respectively. Analogously, they increase rapidly in the early stage and relatively slow in the late stage, the increments in first 7 days are 14.34 g and 17.67 g thus reach 76.78% and 82.82% of their total increments on day 60.

3.2 Strength

3.2.1 Quasi-static compressive strength

The quasi-static compressive strength is an important mechanical performance index to measure the concrete's bearing capacity. Starting from the concrete began to service, quasi-static load always accompanying until the concrete out of work. In this paper, according to the Standard, the hydraulically driven test system was used to compression test with the loading rate of 0.5~0.8 MPa/s.

The quasi-static compressive strength of specimens that when the maintenance finishing is 32.73 MPa, and the results of quasi-static test are listed in Table 3.

Table 3 illustrates that, the quasi-static compressive strength in group N continuously increases, and the growth rate reaches 30.31% on day 60; but for the specimens in group S1 and group S2, their quasi-static compressive strength both increase first and then decrease, the maximum growth rate of group S1 and group S2 are 7.52% and 12.71% respectively, but they are only 76.23% and 82.84% of specimens which under normal environment on day 60.

3.2.2 Dynamic compressive strength

The dynamic stress-strain curves is the concentrate expression of dynamic mechanical performance indicators of concrete specimens, their geometrical shapes and characteristics can reflect the accumulation of deformation and evolution of damage characteristics obviously during the whole process of mechanical damage. The dynamic stress-strain curves of three groups that under different impact loadings are illustrated in Fig. 5.

The following verdicts can be obtained from Fig. 5: for the dynamic stress-strain curves of all specimens, with the increase of strain rate (impact speed), the maximum stress monotonously rising, and the descent stage of curve gradually moves to the right on the whole, which indicates that the deformation degree gradually increasing.

Table 3 The static compressive strength of concrete specimens during corrosive period (MPa)

Corrosion time	0 d	15 d	30 d	45 d	60 d
N	32.73	37.64	39.97	41.34	42.65
S1	32.73	35.19	34.23	32.98	32.51
S2	32.73	36.89	36.14	35.93	35.33

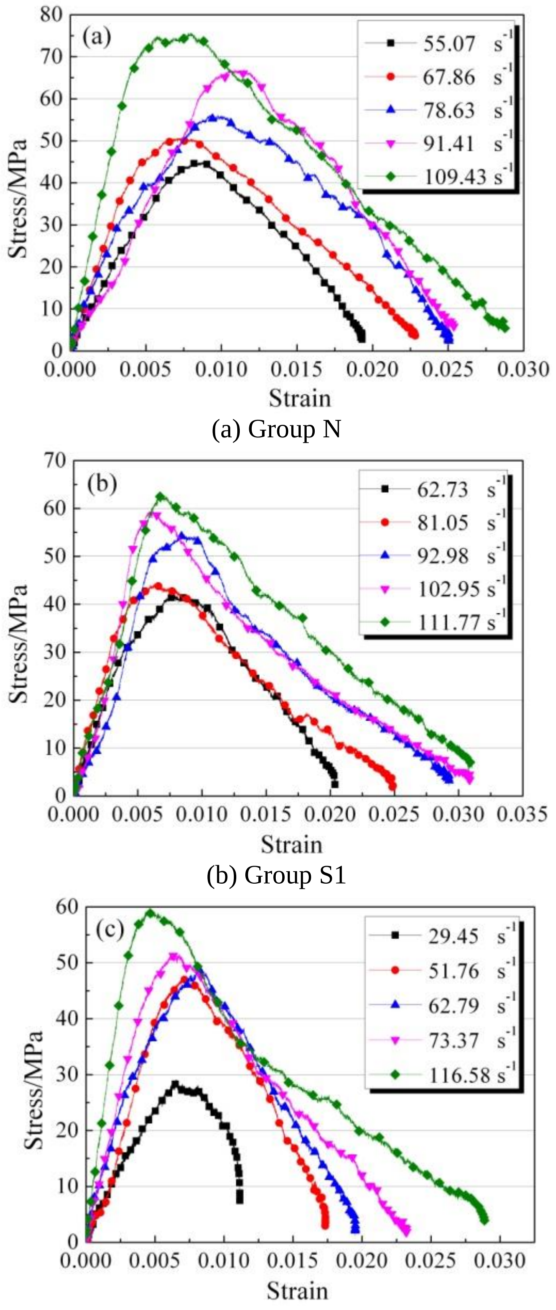

(a) Group N

(b) Group S1

(c) Group S2

Fig. 5 The dynamic stress-strain curves

Dynamic compressive strength $f_{c,d}$, the maximum stress of dynamic stress-strain curves, is an important indicator to measure the effect of loading on strength, and reflects the strength characteristics of the material directly. The relationship between dynamic compressive strength and average strain rate is showed in Fig. 6, from which the following verdicts can be obtained: the dynamic compressive strength is found to be linear to the average strain rate $\bar{\dot{\varepsilon}}$, and the increase ratio of dynamic compressive strength of three groups are diminishingly (the slopes of fitting lines are diminishingly); on the whole, the dynamic compressive strength of group S1 and group S2 have a significant drop when compared with group N, the drop indicates that the endurance of concrete against to dynamic loading is badly affected by the effect of salt corrosion, and the degree of corrosion under chloride environment is more serious than under sulfate environment. The relationship between average strain rate $\bar{\dot{\varepsilon}}$ (s^{-1}) and dynamic compressive strength $f_{c,d}$ (MPa) can be approximately linearly expressed as

$$\text{N:} \quad f_{cd} = 11.7756 + 0.5849\bar{\dot{\varepsilon}} \ (R^2 = 0.9832) \tag{1}$$

$$\text{S1:} \quad f_{cd} = 11.3548 + 0.4577\bar{\dot{\varepsilon}} \ (R^2 = 0.9066) \tag{2}$$

$$\text{S2:} \quad f_{cd} = 26.1249 + 0.3173\bar{\dot{\varepsilon}} \ (R^2 = 0.7692) \tag{3}$$

In order to study the deformation characteristics of concrete that under the impact loading, the ultimate strain (*US*), which defined as the strain when the concrete destroyed completely, is quoted in this paper. Fig. 7 shows the relationship between *US* and average strain rate $\bar{\dot{\varepsilon}}$, the picture shows that, the higher the strain rate is, the bigger ultimate strain can be obtained, thus the greater the deformation, which shows a significant strain rate effect; on the whole, when the strain rate is low, the *US* of group N is maximum, while the deformation of specimens in group S1 attains the maximum when the strain rate is high, and for the specimens in group S2 are always minimum whether the strain rate is high or low.

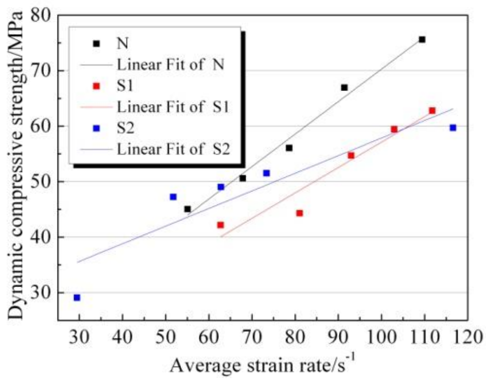

Fig. 6 Dynamic compressive strength

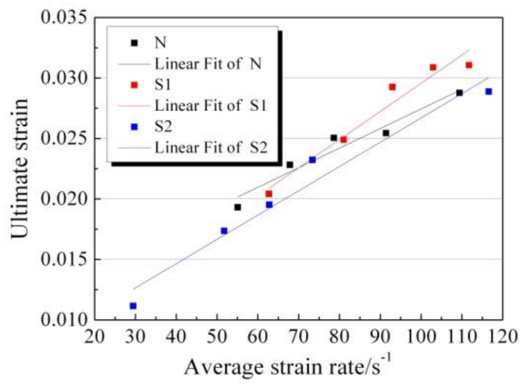

Fig. 7 Ultimate strain

The relationship between average strain rate $\bar{\dot{\varepsilon}}$ (s^{-1}) and *US* can be approximately linearly expressed as

$$\text{N}: US = 0.01125 + 1.6193\times10^{-4}\bar{\dot{\varepsilon}} \quad (R^2 = 0.9284) \tag{4}$$

$$\text{S1}: US = 0.00628 + 2.3283\times10^{-4}\bar{\dot{\varepsilon}} \quad (R^2 = 0.9367) \tag{5}$$

$$\text{S2}: US = 0.00661 + 2.0084\times10^{-4}\bar{\dot{\varepsilon}} \quad (R^2 = 0.9469) \tag{6}$$

3.3 Energy

If there is material, there is energy. Being the most widely used building material, concrete's energy characteristics have always attracted great attention in related area throughout the whole world. Specific energy absorption (*SEA*) is an important mechanical performance indicator from which can measure the ability of material that absorb the external impact energy, the higher the *SEA*, the stronger the ability of absorb impact energy, its physical meaning is the absorption of stress wave energy for per unit volume of concrete, and can be expressed as

$$SEA = \frac{AEc}{A_s l_s}\int_0^T[\varepsilon_i^2(t) - \varepsilon_r^2(t) - \varepsilon_t^2(t)]dt \tag{7}$$

Where A, A_s are cross-sectional areas of bars and specimen, respectively; E is Young's modulus of bars; c is wave velocity in bars; l_s is original length of specimen; T is the time when concrete specimen eventually fails with catastrophic damage; ε_i, ε_r, ε_t are incident, reflected and transmitted strain, respectively.

Fig. 8 shows the *SEA* of specimens in each group under impact loading. The picture illustrated that, same as $f_{c,d}$, with the increase of average strain rate, the *SEA* keep rising, and on the whole, the *SEA* of group N is always maximum, and unlike the $f_{c,d}$, when the strain rate is low, the *SEA* of group S1 is lower than group S2, while it turns out to be higher than group S2 when the strain rate is high. The relationship between average strain rate $\bar{\dot{\varepsilon}}$ (s^{-1}) and *SEA* can be approximately linearly expressed as

$$\text{N}: SEA = -188.4866 + 12.7601\bar{\dot{\varepsilon}} \quad (R^2 = 0.9828) \tag{8}$$

$$\text{S1}: SEA = -188.4176 + 10.2266\bar{\dot{\varepsilon}} \quad (R^2 = 0.9085) \tag{9}$$

$$\text{S2}: SEA = 71.2918 + 6.8194\bar{\dot{\varepsilon}} \quad (R^2 = 0.9221) \tag{10}$$

3.4 Analysis and discussion

The essential of corrosion for concrete is the change of macroscopic and microscopic characteristic inside concrete which result from the reactions of internal structure. After concrete hardened, the cement paste is composed of cement hydration products, unhydrated cement particle, free water and air, etc. The major components of hydration products are calcium hydroxide (crystal), calcium silicate hydrates (gel), calcium ferrite hydrates (gel), calcium aluminate hydrates (crystal) and calcium sulfoaluminate hydrates (crystal), and the content of calcium silicate hydrates which plays a decisive role in concrete strength, is more than 50%.

When the concrete specimens soaked in $NaCl$ solution, the chloride ions penetrated in concrete mainly through three ways: (1) diffusion, the transmission caused by concentration difference of chloride ions; (2) seepage, the chloride ions move into concrete that under the action of water pressure; (3) capillary adsorption, the chloride ions move into concrete together with capillary water with the help of moisture gradient which caused by the function of negative pressure adsorption of capillaries inside the concrete. The chloride ions inside the concrete react with $Ca(OH)_2$ first, and create $CaCl_2$, and then react with calcium aluminate hydrates, create $3CaO{\cdot}Al_2O_3{\cdot}3CaCl_2{\cdot}31H_2O$ which has larger volume. The main reactions (Suryavanshi and Swamy 1996) can be listed as follows

$$3(CaO\cdot Al_2O_3) + 6H_2O \rightarrow 3CaO\cdot Al_2O_3\cdot 6H_2O \tag{11}$$

$$Ca(OH)_2 + 2Cl^- \rightarrow CaCl_2 + 2OH^- \tag{12}$$

$$\begin{aligned}&2Ca(OH)_2 + 2Cl^- + (n-1)H_2O\\ &\rightarrow CaO\cdot CaCl_2\cdot nH_2O + 2OH^-\end{aligned} \tag{13}$$

$$\begin{aligned}&3CaO\cdot Al_2O_3\cdot 6H_2O + 3CaCl_2 + 25H_2O\\ &\rightarrow 3CaO\cdot Al_2O_3\cdot 3CaCl_2\cdot 31H_2O\end{aligned} \tag{14}$$

The impact of sulfate on concrete mainly includes two aspects: on the one hand, when the SO_4^{2-} moves into concrete, it will change into the crystal because of temperature decreasing, and fill in the internal porosity; on the other hand, the sulfate ions inside the concrete react with calcium hydroxide and calcium aluminate hydrates, and create ettringite ($3CaO{\cdot}Al_2O_3{\cdot}3CaSO_4{\cdot}32H_2O$) and gypsum ($CaSO_4{\cdot}2H_2O$).

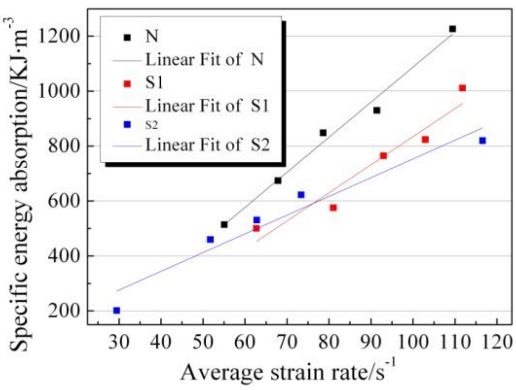

Fig. 8 Specific energy absorption

The main reactions (William *et al*. 1996) can be listed as follows

$$CaO \cdot H_2O + Na_2SO_4 + 2H_2O \rightarrow CaSO_4 \cdot 2H_2O + 2NaOH \tag{15}$$

$$3CaO \cdot Al_2O_3 + 3(CaSO_4 \cdot 2H_2O) + 26H_2O \rightarrow 3CaO \cdot Al_2O_3 \cdot 3CaSO_4 \cdot 32H_2O \tag{16}$$

$$CaO \cdot Al_2O_3 + 3(CaSO_4 \cdot 2H_2O) + 2Ca(OH)_2 + 24H_2O \rightarrow 3CaO \cdot Al_2O_3 \cdot 3CaSO_4 \cdot 32H_2O \tag{17}$$

$$3(CaO \cdot Al_2O_3) \cdot CaSO_4 + 8CaSO_4 + 6CaO + 96H_2O \rightarrow 3(3CaO \cdot Al_2O_3 \cdot 3CaSO_4 \cdot 32H_2O) \tag{18}$$

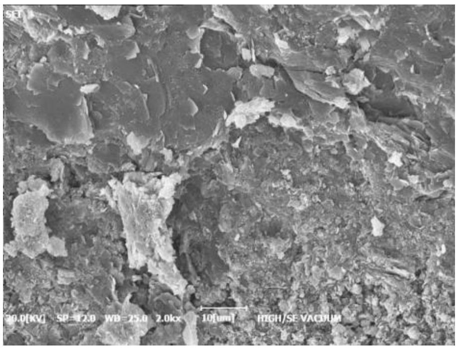
(a) Group N

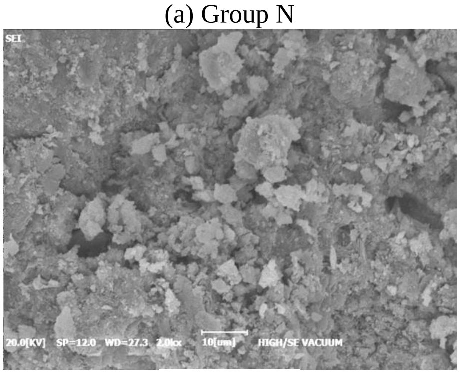
(b) Group S1

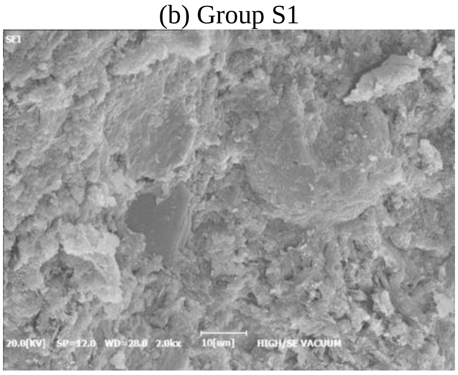
(c) Group S2

Fig. 9 Micro-structure of specimens

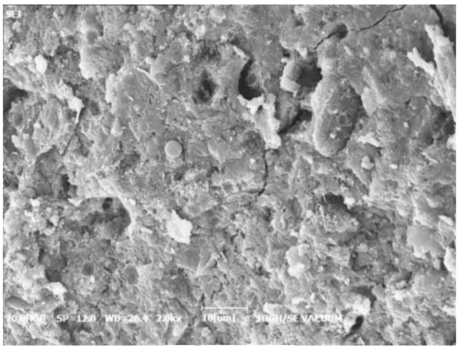
(a) Group N

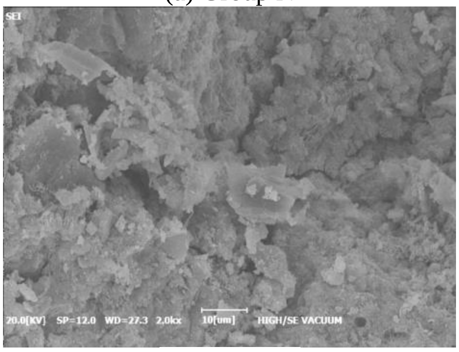
(b) Group S1

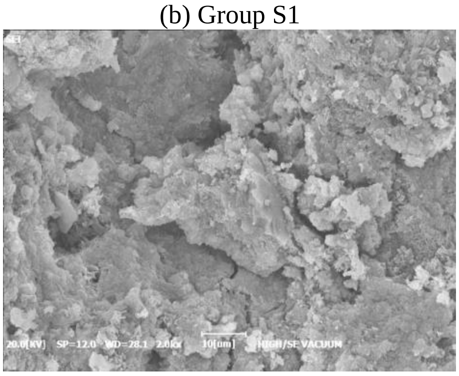
(c) Group S2

Fig. 10 Micro-crack of specimens

3.4.1 Analysis of mass change

For the specimens immersed in chloride and sulfate solution, the increase of mass is mainly caused by two parts, one is the water that has been absorbed during the period of immersion, the other one is the increase of reactions between erosion ions and concrete, and combined with the free water at the same time. So after 60 days corrosion, the mass loss was not exhibited by the specimens in group S1 and group S2, and there was a certain increase of mass instead. What calls for attention is that, the two parts are influence mutually, firstly, the water absorbed in first part can provided as reactants for the second part, and thus gives rise to more water will be absorbed, for the second part, because the larger volume of products, the space inside the concrete will be decreased, and thus affects the water absorption in the first part.

For the specimens in group N, the decrease of mass is mainly because of the moisture loss which includes two parts: the consumption of hydration reaction inside the concrete and water evaporates. Even though the strength of

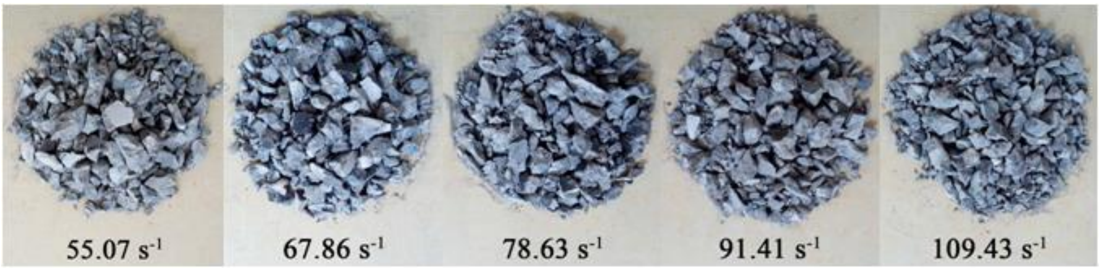

(a) Group N

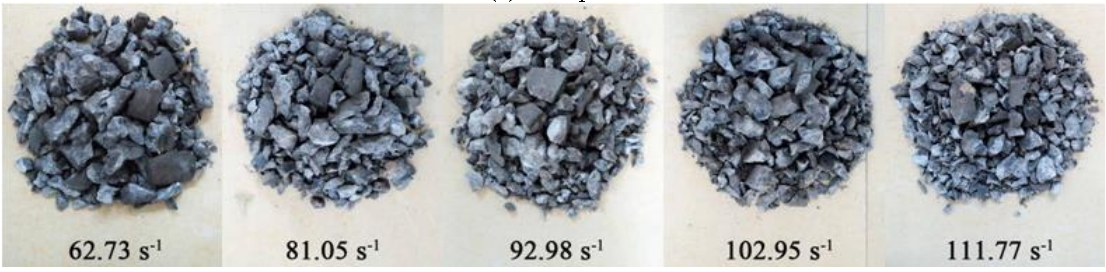

(b) Group S1

(c) Group S2

Fig. 11 Failure forms

concrete after standard curing for 28 days can reach more than 80% of design strength, the hydration reaction inside the concrete is not over yet, and it will be continues and more and more slowly as time goes on; water evaporates is the main part of moisture loss, it often happens on the shallow part of specimens, the water evaporates inside concrete via interior pore which has a greater loss in the early phase of experiment and fewer in later.

3.4.2 Analysis of strength

The quasi-static and dynamic compressive strength of concrete in group S1 and group S2 are significantly decreased during corrosive period. The essential of corrosion is the process of macroscopic and microscopic characteristic changes inside the concrete which result from the changes of internal structure. Cl^{-1} inside the concrete reacts with $Ca(OH)_2$ first, and forms $CaCl_2$, then reacts with calcium aluminate hydrates, forms $3CaO{\cdot}Al_2O_3{\cdot}3CaCl_2{\cdot}31H_2O$ which has relatively large volume and low strength; SO_4^{2-} inside the concrete reacts with calcium hydroxide and calcium aluminate hydrates, and forms ettringite ($3CaO{\cdot}Al_2O_3{\cdot}3CaSO_4{\cdot}32H_2O$) and gypsum ($CaSO_4{\cdot}2H_2O$), due to the consumption of water, certain amounts of sodium sulfate crystals are formed, which fill in internal pores of concrete.

It is known that, there are some initial holes inside concrete, in the initial reaction period, the reaction products are relatively few, and they are filling in the initial holes, as pointed in Chen's work (2008), so there is no internal stress at this time, and it has a positive effect on strength, as seen in Table 3. While with the increase of corrosion time, the products grows and touches to the boundary of the initial holes, on the one hand, due to the consumption of chemical reactions, the original hydration products have changed, thus the internal composition and structure of concrete were destroyed. On the other hand, the volume expansion of excess products causes internal stress, which has an internal damage to the structure of concrete, and under the action of internal stress, the internal composition and structure of concrete are destroyed, the properties of original hydration products are changed, which leads to the decrease of concrete strength, as seen in Table 3.

Figs. 9 and 10 are microstructure and micro-crack of specimens in each group, from which the following messages can be obtained: because there is no corrosion to specimens in group N, as the corrosion time goes on, the hydration product of *C-S-H* is continuously increasing, so is their compactness, and the cracks inside them are small in size and less in number, thus their strength increases continually; while for the specimens in group S1 and S2, There are many flocculation crystals which are closely spaced, and form a dense crystal layer inside the corroded specimens, this will result in internal stress, and under the force of the stress, the size of internal cracks becomes larger, and leads to the performance degradation of these specimens.

The dynamic compressive strength increases with the increase of strain rate, mainly because of the prominent strain rate effect (Ross *et al*. 1996, Grote *et al*. 2001, Zhou and Hao 2008, Su and Xu 2013), meanwhile, as Fig.11 shows, with the increase of impact velocity (strain rate), the degree of damage tend to be more serious gradually, which can be expressed in the increase of number and the decrease of size of the fragment.

As shown in Fig. 6 and the analysis above, because of the specimen in group S1 has a more porous structure after corroded, it has a higher dynamic compressive strength than the specimen in group S2. What's more, after corroded by sulfate solution, the volume of products is larger than that of products corroded by chloride solution, which means the lesser size of internal deformable space, thus the strain of specimen in group S2 always keeps minimum. Varying in a certain range, the higher the strength, the greater the strain, thus the strain of specimen in group N is maximum when the strain rate is low. Because of the strain rate effect, the strain is linear to the average strain rate, while the increase ratio (the slop of fitted line) of group N is smaller than other two groups, maybe it is results from the interaction of the effect of strain rate and corrosion.

3.4.3 Analysis of SEA

From a perspective of fracture mechanics, the failure of concrete is mainly because of the initiation and extension of cracks. There are many kinds of energy during the failure process (Labuz and Dai 2000, Fengnian *et al*. 2004), and the primary of them are elastic potential energy, surface energy, plastic potential energy, radiant energy and kinetic energy, etc.

There are two factors that have an effect on the capability of energy absorption of concrete, one is the strength of concrete itself, the higher the strength is, the more external impact loading it can offset, that the stronger the capacity of energy absorption, after attacked by erosion ions, the concrete strength has declined, and so as the resistance to impact loading, thus the capability of energy absorption has been weakened; the other factor is the size of deformable space inside the concrete, the larger the internal porosity has, the more room for the deformation of concrete that under dynamic loading, thus the stronger the capability of energy absorption which depends on deformation. When the strain rate is low, the strength of concrete in group S1 is higher than group S2, the former plays the major role, and the *SEA* of group S1 is higher than group S2; while the latter plays the major role when the strain rate is high, because of the internal porosity of specimens in group S2 is filled with sodium sulfate crystal, ettringite and gypsum, the size of deformable space inside the concrete is smaller than group S1, thus the capability of energy absorption is weaker.

4. Conclusions

The hydraulically driven test system and Φ 100 mm split Hopkinson pressure bar (SHPB) test device were employed to research the quasi-static and dynamic mechanical properties of concrete specimens which has been immersed in $NaCl$ and Na_2SO_4 solutions both with the mass fraction of 15% for a period of 60 days. The main conclusions and findings in this paper are as the following:

- For the specimens in group N, because of the evaporation of free water and the hydration of cement, the mass present the law of continuous declination, it declines rapidly in the early stage and relatively slow in the late stage, the loss of mass after soaked for one week is 61.48% of the total loss on day 60. But for the specimens in group S1 and group S2, because of the combined action of water absorption and corrosion, their mass displayed the law of increase gradually with the increase of time, the increments in first 7 days are 14.34 g and 17.67 g, thus reach 76.78% and 82.82% of the total increments which are 0.79% and 0.91% of their specimen's weight on day 60, and both increase relatively slow in the late stage.
- During the corrosive period, the quasi-static compressive strength of group S1 and group S2 both increase first and then decrease, the maximum growth rate of them are 7.52% and 12.71% respectively, but they are only 76.23% and 82.84% of specimens which under normal environment on day 60.
- After immersed for 60 days, there were different decrease to dynamic compressive strength and specific energy absorption, and so as their strain rate sensitivities; on the whole, when the strain rate is low, the capability of energy absorption of group S2 is stronger than group S1, while it turns out to weaker when the strain rate is high.

Acknowledgments

This work was sponsored by the foundation items below:

Projects of National Natural Science Foundation of China (51208507; 51378497);

Industrial Public Relation Project for Science and Technology Development in Shanxi Province of China (2014K10-15);

Supported by the Fund of the State Key Laboratory of Disaster Prevention & Mitigation of Explosion & Impact (PLA University of Science and Technology) (DPMEIKF201406);

Projects of Youth Technology New Star of Shanxi Province in China (2013KJXX-81);

Doctorate Fellowship Foundation of Air Force Engineering University (kgd082314005).

References

Abdelmseeh, V.A., Jofriet, J. and Hayward, G. (2008), "Sulphate and sulphide corrosion in livestock buildings, part I: Concrete deterioration", *Biosyst. Eng.*, **99**(3), 372-381.

Chen, J.K., Jiang, M.Q. and Zhu, J. (2008), "Damage evolution in cement mortar duo to erosion of sulphate", *Corros. Sci.*, **50**(9), 2478-2483.

Chindaprasirt, P. and Chalee, W. (2014), "Effect of sodium hydroxide concentration on chloride penetration and steel

corrosion of fly ash-based geopolymer concrete under marine site", *Constr. Build. Mater.*, **63**, 303-310.
Cho, H.C., Lee, D.H., Ju, H., Kang, S.K., Kim, K.H. and Monteiro, P.J.M. (2015), "Remaining service life estimation of reinforced concrete buildings based on fuzzy approach", *Comput. Concrete*, **15**(6), 879-902.
Clifton, J.R. and Ponnersheim, J.M. (1994), *Sulfate Attack of Cementitious Materials: Volumetric Relations and Expansions*, NIST IR, 5390.
Cohen, M.D. and Mather, B. (1991), "Sulfate attack on concrete: Research needs", *ACI Mater. J.*, **88**(1), 62-69.
Crammond, N.J. (2003), "The thaumasite form of sulfate attack in the UK", *Cement Concrete Comp.*, **25**(8), 809-818.
Dallaire, E., Aitein, P.C. and Laehemi, M. (1997), *An Example of the Use of Reactive Powder Concrete: The Sherbrooke Pedestrian Bikeway Bridge*, Technology Transfer Day: The Specifications and Use of HPC, Toronto, Canada.
Deby, F., Carcassès, M. and Sellier, A. (2009), "Robabilistic approach for durability design of reinforced concrete in marine environment", *Cement Concrete Res.*, **39**(5), 466-471.
Fei, F.L., Hu, J., Wei, J.X., Yu, Q.J. and Chen, Z.S. (2014), "Corrosion performance of steel reinforcement in simulated concrete pore solutions in the presence of imidazoline quaternary ammonium salt corrosion inhibitor", *Constr. Build. Mater.*, **70**, 43-53.
Frew, D.J., Forrestal, M.J. and Chen, W. (2002), "Pulse shaping techniques for testing brittle materials with a split Hopkinson pressure bar", *Exp. Mech.*, **42**(1), 93-106.
Gama, B.A. (2014), *Split Hopkinson Pressure Bar Technique: Experiments, Analyses and Applications*.
Gao, J., Yu, Z., Song, L., Wang, T. and Wei, S. (2013), "Durability of concrete exposed to sulfate attack under flexural loading and drying-wetting cycles", *Constr. Build. Mater.*, **39**, 33-38.
Grote, D.L., Park, S.W. and Zhou, M. (2001), "Dynamic behavior of concrete at high strain rates and pressures: I. Experimental characterization", *J. Impact. Eng.*, **25**(9), 869-886.
Hossain, K.M.A. and Lachemi, M. (2006), "Performance of volcanic ash and pumice based blended cement concrete in mixed sulfate environment", *Cement Concrete Res.*, **36**(6), 1123-1133.
Jin, F., Jiang, M. and Gao, X. (2004), "Defining damage variable based on energy dissipation", *Chin. J. Rock Mech. Eng.*, **23**(12), 1976-1980.
Labuz, J.F. and Dai, S.T. (2000), "Residual strength and fracture energy from plane-strain testing", *J. Geotech. Geoenviron. Eng.*, **126**(10), 882-889.
Li, W.M. and Xu, J.Y. (2009), "Pulse shaping techniques for large-diameter split hopkinson pressure bar test", *Acta Armamentarii*, **30**(3), 350-355.
Lu, F., Forrestal, M.J., Chen, W. and Frew, D.J. (2002), "Dynamic compression testing of soft materials", *J. Appl. Mech.*, **69**(3), 214-223.
Ravichandran, G. and Subhash, G. (1994), "Critical appraisal of limiting strain rates for compression testing of ceramics in a split hopkinson pressure bar", *J. Am. Ceram. Soc.*, **77**(1), 263-267.
Ross, C.A., Jerome, D.M., Tedesco, J.W. and Hughes, M.L. (1996), "Moisture and strain rate effects on concrete strength", *ACI Mater. J.*, **93**(3), 293-300.
Roventi, G., Bellezze, T., Giuliani, G. and Conti, C. (2014), "Corrosion resistance of galvanized steel reinforcements in carbonated concrete: Effect of wet-dry cycles in tap water and in chloride solution on the passivating layer", *Cement Concrete Res.*, **65**, 76-84.
Sharmila, P. and Dhinakaran, G. (2015), "Strength and durability of ultra fine slag based high strength concrete", *Struct. Eng. Mech.*, **55**(3), 675-686.
Song, H. and Chen, J. (2011), "Effect of damage evolution on poisson's ratio of concrete under sulfate attack", *Acta Mech. Sol. Sin.*, **24**(3), 209-215.
Song, Z., Jiang, L. and Zhang, Z. (2017), "Chloride diffusion in concrete associated with single, dual and multi cation types", *Comput. Concrete*, **17**(1), 53-66.
Steinberg, E. (2009), "Structural reliability of prestressed UHPC Flexure models for bridge girders", *J. Brid. Eng.*, **15**(1), 65-72.
Su, H. and Xu, J. (2013), "Dynamic compressive behavior of ceramic fiber reinforced concrete under impact load", *Constr. Build. Mater.*, **45**, 306-313.
Suryavanshi, A.K. and Swamy, R.N. (1996), "Stability of friedel's salt in carbonated concrete structural elements", *Cement Concrete Res.*, **26**(5), 729-741.
Tanyildizi, H. (2017), "Prediction of compressive strength of lightweight mortar exposed to sulfate attack", *Comput. Concrete*, **19**(2), 217-226.
Türkmen, İ. and Gavgalı, M. (2003), "Influence of mineral admixtures on the some properties and corrosion of steel embedded in sodium sulfate solution of concrete", *Mater. Lett.*, **57**(21), 3222-3233.
Uysal, M., Yilmaz, K. and Ipek, M. (2012), "The effect of mineral admixtures on mechanical properties, chloride ion permeability and impermeability of self-compacting concrete", *Constr. Build. Mater.*, **27**(1), 263-270.
William, G.H. and Bryant, M. (1999), ""sulfate attack," or is it?", *Cement Concrete Res.*, **29**(5), 789-791.
Yang, K.H., Cheon, J.H. and Kwon, S.J. (2017), "Modeling of chloride diffusion in concrete considering wedge-shaped single crack and steady-state condition", *Comput. Concrete*, **19**(2), 211-216.
Ye, H., Jin, X., Chen, W., Fu, C. and Jin, N. (2017), "Prediction of chloride binding isotherms for blended cements", *Comput. Concrete*, **17**(5), 683-702.
Yin, G., Zuo, X., Tang, Y., Ayinde, O. and Ding, D. (2017), "Modeling of time-varying stress in concrete under axial loading and sulfate attack", *Comput. Concrete*, **19**(2), 143-152.
Yoon, I.S. and Nam, J.W. (2017), "New experiment recipe for chloride penetration in concrete under water pressure", *Comput. Concrete*, **17**(2), 189-199.
Zhou, X.Q. and Hao, H. (2008), "Modelling of compressive behaviour of concrete-like materials at high strain rate", *J. Sol. Struct.*, **45**(17), 4648-4661.
Zuo, X., Wang, J., Sun, W., Li, H. and Yin, G. (2017), "Numerical investigation on gypsum and ettringite formation in cement pastes subjected to sulfate attack", *Comput. Concrete*, **19**(1), 19-31.

CC